INVESTIGATION OF STRESS ANALYSIS ON COATING-SUBSTRATE INTERFACIAL WITH PRE-CRACKED MODEL

MOHAMAD ZULFADLI BIN MOHAMAD RANI

A project report in partial
fulfillment of the requirements for the award of the
Degree of Master of Mechanical Engineering

Faculty Mechanical and Manufacturing Engineering
University Tun Hussein Onn Malaysia

JANUARY 2014

ABSTRACT

This study is intended to predict the stress behavior of thick hard coating at the interface with the changes of coating stiffness and thickness to the substrate of Ti-6Al-4V and SCMV. The elastic mismatch between the coating and the substrate is presented in the value of Dundur's parameter α. The prediction is done using simple geometry of a cylinder-on-flat model in 2D analysis subjected to normal and tangential loading. Tangential stress distribution along the coating-substrate interface is then obtained from the FE modelling after a finite sliding of the cylinder. It is predicted that the maximum tangential stress value predicted at the interface which relates to coating fracture failure is increasing as stiffer coating is used on compliant substrate (i.e. increasing α values). The location of the maximum tangential stress predicted also changes from the trailing edge to the center of contact with increasing α values. Thus, evolution of stress intensity factor at crack tip, which highly depends on tangential stress distribution, was studied. A pre-micro-crack was placed at the coating-substrate interface to study the effect of stress intensity factor on stress behavior at crack tip. The stress intensity factor at crack tip does not exceed the fracture toughness due to null face friction applied to the crack seam. Effect of changes of coating thickness on the predicted maximum tangential stress value is more significant for high positive α values. Risk of coating fracture at the interface is therefore predicted to increase with the increase of coating thickness and stiffness.

ABSTRAK

Kajian ini adalah bertujuan untuk meramal daya tahan tekanan pada antara-lapis (interface) salutan yang keras dan tebal dengan perubahan kekukuhan dan ketebalan saduran kepada substrat Ti- 6AL- 4V dan SCMV . Ketidaksepadanan ciri elastik antara saduran dan substrat diistilahkan dalam nilai parameter Dundur α Dundur. Kajian dilakukan dengan menggunakan geometri mudah, silinder dan blok-rata dalam analisis 2D yang tertakluk kepada bebanan yang normal dan melintang (tangen). Agihan tegasan tangen di sepanjang antara-lapis; kemudiannya diperoleh daripada model FE selepas gerakan melintang oleh geometri silinder. Diramalkan bahawa nilai tegasan tangen maksimum yang dijangka pada antara-lapis yang berkaitan dengan daya-tahan patah saduran semakin meningkat kerana saduran yang lebih keras digunakan pada substrat (iaitu nilai α yang lebih positif). Lokasi tegasan tangen maksimum meramalkan juga perubahan dari belakang sentuhan ke pusat sentuhan dimana berlakunya peningkatan nilai α . Satu rekahan permulaan berskala mikro diletakkan di antara-muka saduran dan substrate untuk mengkaji tentang foktor keamaatan tegasan di hujung rekahan. Oleh itu, evolusi tentang faktor keamatan tegasan di hujung retak, yang sangat bergantung kepada agihan tegasan tangen, telah dikaji. Didapati bahawa faktor keamatan tegasan di hujung rekahan tidak melebihi nilai daya-tahan patah saduran kerana nilai pekali geseran pada muka rekahan diambil kira sebagai sifar (0). Kesan perubahan ketebalan saduran pada nilai tegasan tangen yang maksimum juga meramalkan, adalah lebih penting bagi nilai-nilai α positif yang lebih tinggi. Oleh itu, risiko keretakan saduran pada antara-lapis dijangka meningkat dengan peningkatan ketebalan saduran dan ketegangannya.

CONTENTS

LIST OF TABLES

LIST OF FIGURES

LIST OF SYMBOLS AND ABBREVIATIONS

K , K_σ	-	Stress intensity factor
K_I	-	Stress intensity factor on *Mode-I*
K_{IC}	-	Fractur Toughness
α	-	Dundur's Parameter on elastic mismatch
β	-	Dundur's Parameter on Poisson's Ratio difference
σ	-	Tensile Stress
τ	-	Shear Stress
θ	-	Angle
E	-	Young's Modulus
ν	-	Poisson's Ratio
μ	-	Symbol of friction of coefficient
F	-	Force
σ_{xx}	-	Stress acted on x-plane
COF		Coefficient of Friction
Mode-I		Mode I crack opening
SIF		Stress Intensity Factor
SCMV		High strength steel (HSS)
Ti-6AL-4V		Titanium alloy
MPa		Mega Pascal
CPRESS		Contact pressure
LEFM		Linear elastic fracture mechanics

CHAPTER 1

INTRODUCTION

1.1 Background Study

A coating is a covering that is applied to the surface of an object, which also called substrate. In many cases, coatings were applied to improve surface properties of substrate, such as appearance, adhesion, water resistance, corrosion resistance, wear resistance, and scratch resistance. Within few years back, some of new coatings made using nanotechnology promises to give a long-life surface protection. In some other cases, coating also used in printing processes and electronic parts fabrication where the coating forms an essential part of the finished product.

Ceramic coatings are in wide use nowadays. The capability of this coatings to reduce friction due to contact stresses and wear resistance had made it as a great choice to be used as protection for surfaces that are subjected to contact loading. Examples include machine tools, cams and followers, piston rings, valves and bearings. In all these applications, failure of the coating is a concern. The relatively high hardness and inertness of ceramic coating properties makes this type of coating of interest for protection of substrate materials against corrosion, oxidation and wear. In particular, the use of such coatings on machine tools can extend the life of these items by several orders of magnitude.

Coatings that used to lubricate a substrate called lubricants coating which also known as solid film lubricants coating. It provides a lubricating film that reduces

friction, inhibits galling and seizing and in some instances can aid in dispersing heat. It's slippery and provides an extremely low coefficient of friction. In automotive or aero engineering, one of the obvious reasons for using a lubricating coating is to reduce friction, which improves wear, extends parts life and free up horse power normally lost to friction. A second major benefit is a reduction in part temperature. This is especially important to such parts as valve spring. Here, the choice of coating is critical as certain ingredients of the coating can trap heat in parts.

1.2 Problem Statement

To make a component with long operational life, low level of friction need to be achieved as it will results in lower stress magnitude. Increased hardness of the coating will make it to be wear resist, but in the same time it will increase the coating brittleness and prone to brittle-type fracture.

The presence of coating has second important effect. Many coatings does not bond well to their substrates. The interface between layer and substrate contains flaws, and the coating layer generally has a fracture toughness. Consequently, the coating may fracture from the at the coating-substrate interface under contact loading. Cracking may be initiated from flaws just above the interface itself and subsequently caused a catastrophic failure on the coating layer.

Stress distribution on the coating interface makes a primary parameter to determine the toughness of a coating that will soon failed. The toughness of a coating should bare some stress which induced by a severe load that could break the coating in several modes of crack opening. Stress intensity factor plays an important role by determining the level to which the material can bare a load in the presence of crack with the magnitude of cracking which can be tolerated at a specific stress level.

1.3 Objectives of study

To solve the problems stated, some objectives has been made to guide this project.

- To simulate finite element (FE) analysis of stress distribution for a coated substrate when subjected to contact loading.
- To investigate the effect of mechanical properties, friction coefficient and thickness to the stress distribution at coating interface.

- To investigate the stress intensity factor for a pre-micro crack originated from the coating-substrate interface.

1.4 Scope of study

The modeling effort of coated substrate has been done by using ABAQUS finite element software. The material model for substrate was high strength steel, SCMV and Titanium Alloy, Ti-6Al-4V which is an aero engine specific. The finite element modeling was done in two-dimensional.

The load applied to the geometry is between 500 N/mm with an applied displacement of 100 micron, which will result a complete sliding of the contact.
A pre-cracked finite element model has been simulated to investigate tangential stress distribution on the coating of coated substrate. Initial pre-crack will take place at the interface of coating and positioned perpendicular to it of a size of 7.5 μm to study the stress intensity factor, *K*. The contact was based on a simple round and flat contact configuration with contact semi-width of around 190 μm – 250 μm. The parameters that were considered to investigate the effect of crack propagation in coating was:

- The friction coefficient were varied from 0.1 to 0.9 to simulate the friction force effect.
- Mechanical properties of the coating such as stiffness of coating will be varied around 100-200 GPa.
- The coating thickness were varied between 100-200 μm which means a thick coating is used

CHAPTER 2

LITERATURE REVIEW

2.1 Introduction

Thin and hard layer of coatings have been increasingly used currently in engineering applications, which is mainly to reduce the effect of wear and friction. Ceramic coatings has presented interesting mechanical properties of surface loading applications such as high hardness, inertness of chemical reactions, stiffer behavior, and highly wear resist. The advancement of coatings technology allowed the deposition of coating films that would not be viable to the years back then. As generally known; thickness of coating, hardness of coating, and modulus of elasticity plays an important role to control the number the deformation of the crack. Other than that, the Hertzian theory is only valid for homogeneous material. Thus, it cannot be directly used for the case of different properties between coating and substrate.

2.2 Stress-Strain

Stress-strain relationship or constitutive equations are essential in engineering design and analysis. For example, elastic behavior of a material with an elastic stress-strain relationship is assumed and used in calculating stresses and deflections in simple components; such as beams or shafts. Some other components with a relative complex geometry and loading may be analyzed by using the same basic

assumptions with the use of theory of elasticity. This sub-topic will discuss systematically from the elementary level of Stress and Strain concepts through the usage of Principle Strains in analysis.

2.2.1 Stress

It is defined as load P per unit area which acting on a surface as in Equation 2.1. The theory is similar to pressure but it can be either tensile stress (positive value) or compressive (negative value). Stress acted on a surface are not necessarily to be normal to it; which it could be normal stress σ or shear stress τ. Shear stress carries the same definition as normal stress but in a different manner which the force F is acted tangentially with respect to the surface as shown in Equation 2.2.

$$\sigma = \frac{P}{A} \tag{2.1}$$

$$\tau = \frac{F}{A} \tag{2.2}$$

Normal stress σ, is acted perpendicular to the surface while shear stress τ is acted tangentially to the surface. Figure 2.1 shows the relationship between normal and tangential stress acted on a surface. P and F denotes the normal and tangential stress on a surface which resulting in R.

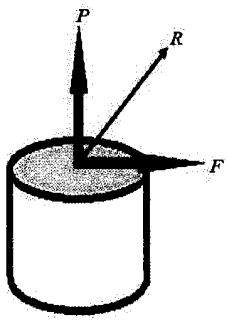

Figure 2.1: Normal stress and shear stress acted on a surface

2.2.2 Strain

Strain is a measure a material to its ductility behavior. Strain is simply defined as ratio of total deformation ΔL (difference between final length L_f to the initial length L_i) with the initial length L_i of the material body which is being applied by an external forces as shown in Equation 2.3. This definition is simply called *Engineering Strain* or *Cauchy strain*. Figure 2.2 shows how strains works on a material which been exerted with external forces.

$$\varepsilon = \frac{\Delta L}{L_i} = \frac{L_f - L_i}{L_i} \tag{2.3}$$

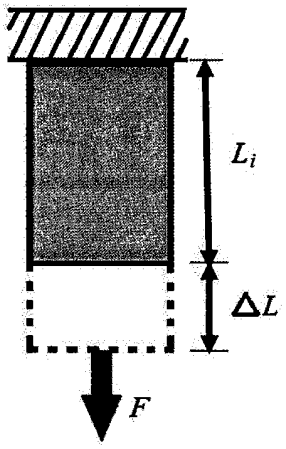

Figure 2.2: Engineering strain on a ductile material

2.2.3 Stress-Strain Relations

There were two types of deformation would take place in a material. One is elastic deformation and another is plastic deformation. Elastic deformation is known when the material is recovered immediately upon unloading at which the stress and strain are usually proportional to each other. In Figure 2.3 shows the relations between stress and strain in an elastic deformation. It can be seen that the deformation results in a linear trend of stress-strain growth, which can be called as linear elastic deformation.

Equation 2.4 as stated below is the *Modulus of Elasticity, E* that corresponds to the constant of that particular proportionality between stress and strain. The value can be obtained as the gradient of linear curve of elastic deformation.

$$E = \frac{\sigma}{\varepsilon} = \frac{\sigma_b - \sigma_a}{\varepsilon_b - \varepsilon_a} \tag{2.4}$$

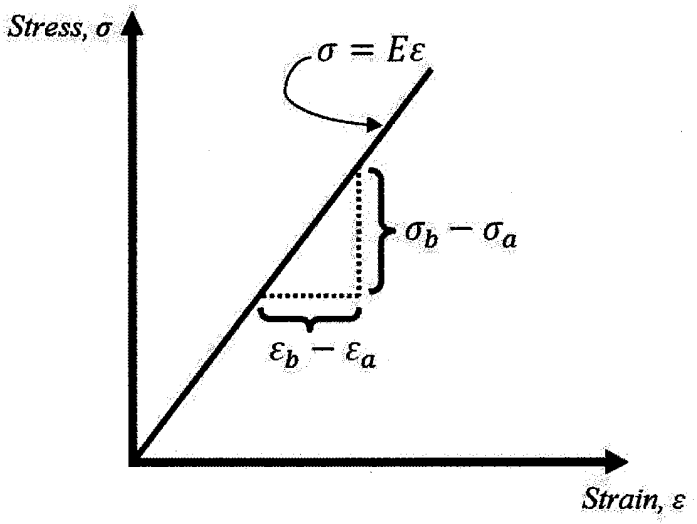

Figure 2.3: Stress-strain relationship of elastic deformation

While in the other hand, plastic deformation does not recover the material shape upon the unloading. Therefore, the shape deformation is permanent. Once plastic deformation begins, only slight increase in stress will usually caused a relatively large additional deformation; which would ease further deformation (yielding). This value of stress where that behavior begins is called *Yield stress* σ_y.

Figure 2.4 shows the relationship between elastic and plastic deformation. Plastic deformation is found to be slightly higher value on plastic strain ε_p if compared with elastic strain ε_e. The total deformation of a single material which exhibits' a full elasto-plastic deformation would have the total strain ε_x.

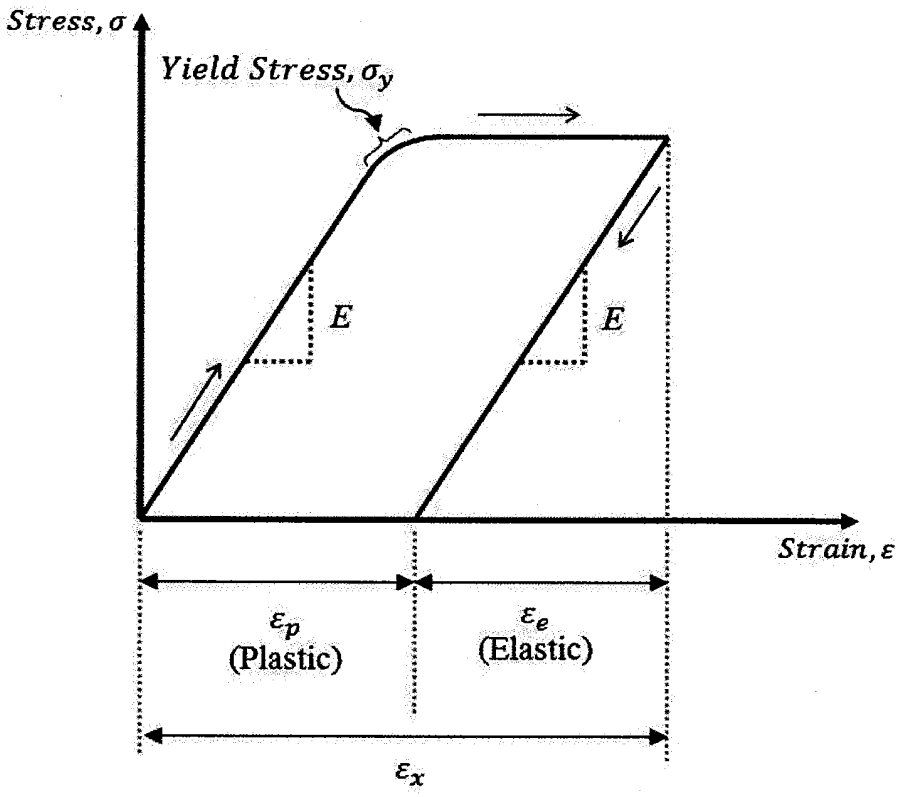

Figure 2.4: The relationship of elasto-plastic deformation

2.2.4 Stresses in three-dimension

A complete description consist of normal stresses in three directions σ_x, σ_y, and σ_z and shear stresses on three planes τ_{xy}, τ_{yz}, and τ_{zx} can be seen in Figure 2.5. By considering the normal stresses first, and assume that small strain theory applies; the strains caused by each component of stress can simply be applied together.

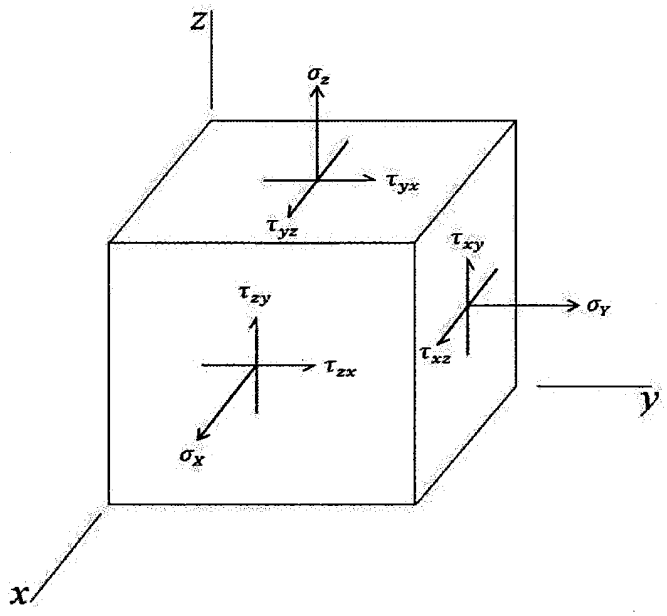

Figure 2.5: Stresses in three-dimensional

A stress in x-direction, σ_x causes a strain in x-direction, $\frac{\sigma_x}{E}$ and also cause a strain in y-direction, $\frac{-\nu\sigma_x}{E} = \varepsilon_y$, and the same strain in z-direction. Thus, Table 2.1 is a result of strain at each direction for both three normal stresses acted in three-dimensional.

Table 2.1: Resulting strains at each x, y, and z-directions

Stress	Strains at each directions		
	x	y	z
σ_x	$\frac{\sigma_x}{E}$	$\frac{-\nu\sigma_x}{E}$	$\frac{-\nu\sigma_x}{E}$
σ_y	$\frac{-\nu\sigma_y}{E}$	$\frac{\sigma_y}{E}$	$\frac{-\nu\sigma_y}{E}$
σ_z	$\frac{-\nu\sigma_z}{E}$	$\frac{-\nu\sigma_z}{E}$	$\frac{\sigma_z}{E}$

(Dowling, 2006)

By adding those every colomns in Table 1, total strain in each direction is given in following Equation 2.5, 2.6, and 2.7.

$$\varepsilon_x = \frac{1}{E}[\sigma_x - \nu(\sigma_y + \sigma_z)] \tag{2.5}$$

$$\varepsilon_y = \frac{1}{E}[\sigma_y - \nu(\sigma_x + \sigma_z)] \tag{2.6}$$

$$\varepsilon_z = \frac{1}{E}[\sigma_z - \nu(\sigma_x + \sigma_y)] \tag{2.7}$$

2.2.5 Plane stress

In general, a three-dimensional stresses consist of six components of stresses, σ_x, σ_y, σ_z, τ_{xy}, τ_{yz}, and τ_{zx}. If three components of stress acting on one of the three pairs of parallel faces of the element are all zero, then a state of plane stress exist. Thus, the unstressed planed is taken to be parallel to the x-y plane would give such in Equation 2.8.

$$\sigma_z = \tau_{zx} = \tau_{yz} = 0 \tag{2.8}$$

The remaining three components of stresses, σ_x, σ_y, and τ_{xy} are as shown in Figure 2.6 on a square element of a material. This square element is simply a cubic element viewed parallel to the z-axis.

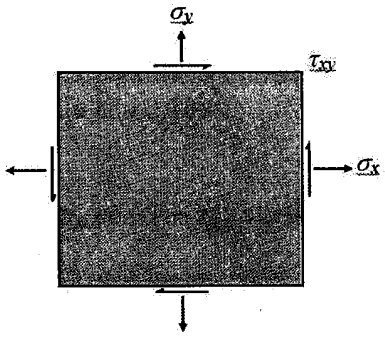

Figure 2.6: Plane stress viewed parallel to the z-axis

As the cubic element in Figure 2.6 rotated in counterclockwise (CCW) direction, a same state may be described but with the other coordinate system (i.e. x'-y') this system is related to the original one but with an angle of rotation θ, and the values of the stress components change to σ'_x, σ'_y, and τ'_{xy}. Those new quantities does not represents a new state of stress but rather equal to the original one as shown in Figure 2.7(a).

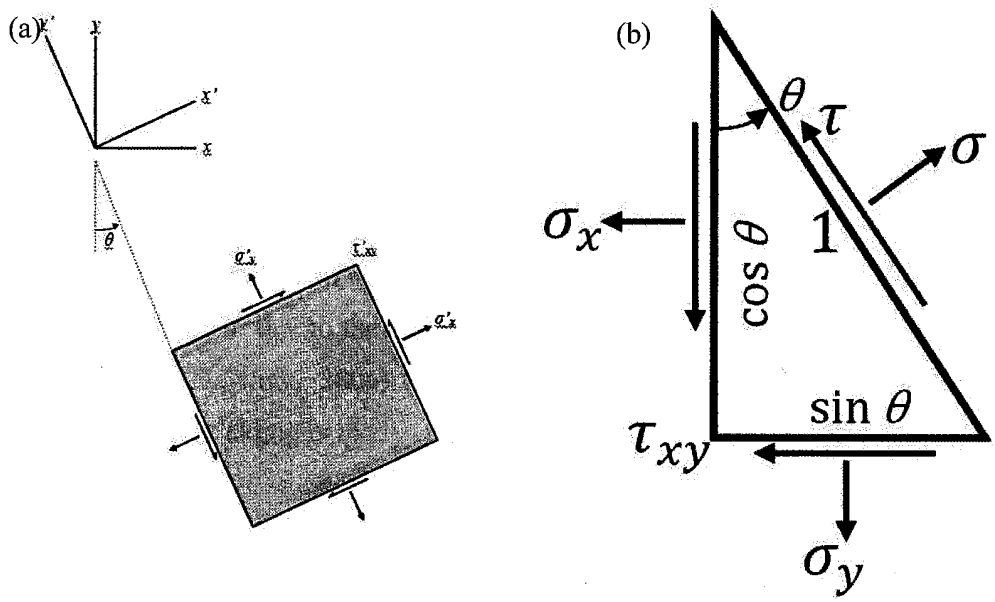

Figure 2.7: Plane stresses with an angle of rotation; (a) the same illustration of the identical state of stress for a rotated coordinate system, and (b) stresses on an slanted plane

From Figure 2.7(b), by summing all forces in x-direction and then in y-direction would gives equation 2.9 and 2.10.

$$\sigma \cos\theta - \tau \sin\theta - \sigma_x \cos\theta - \tau_{xy} \sin\theta = 0 \tag{2.9}$$

$$\sigma \sin\theta + \tau \cos\theta - \sigma_y \sin\theta - \tau_{xy} \cos\theta = 0 \tag{2.10}$$

By solving equation 2.9 and 2.10 for the unknowns of σ and τ with some basic trigonometry identity, gives equation 2.11 and 2.12; which called the

transformation equation. Note that, the angle of rotation θ is positive in counterclockwise (CCW).

$$\sigma = \frac{\sigma_x+\sigma_y}{2} + \frac{\sigma_x-\sigma_y}{2}\cos 2\theta + \tau_{xy}\sin 2\theta \tag{2.11}$$

$$\tau = -\frac{\sigma_x - \sigma_y}{2}\sin 2\theta + \tau_{xy}\cos 2\theta \tag{2.12}$$

2.2.6 Principle stresses

It is defined as the maximum and minimum stress at a given location (Dowling, 2006). The particular plane on which these act are called principle planes with the highest and lowest normal and shear stresses are of interest. As an example, a brittle fracture may occur due to the highest tensile normal stress and yielding is caused by shear stress (Dowling, 2006). Thus, highest value of it is needed to determine whether or not yielding is likely to happen at a given location in a component.

The normal stresses (σ'_x and σ'_y) and the shear stress (τ'_{xy}) vary smoothly with respect to the rotation angle θ, in accordance with the *transformation equations*. There exist a couple of particular angles where the stresses take on special values. First, there exists an angle θ_n where the shear stress τ'_{xy} becomes zero. That angle is found by setting τ'_{xy} to zero in the above shear transformation equation and solving for θ (set equal to θ_n). The result as in equation 2.13.

$$\tan 2\theta_n = \frac{2\tau_{xy}}{\sigma_x - \sigma_y} \tag{2.13}$$

The two angle, θ_n separated by 90° satisfying the relationship. Thus, the maximum and minimum normal stresses are the principal stress as in Equation 2.14;

$$\sigma_1, \sigma_2 = \frac{\sigma_x + \sigma_y}{2} \pm \sqrt{\left(\frac{\sigma_x - \sigma_y}{2}\right)^2 + {\tau_{xy}}^2} \tag{2.14}$$

Another important angle, θ_s, is where the maximum shear stress occurs. This is found by finding the maximum of the shear stress from *transformation equation* and have a first derivative with respect to θ_n, and solving for θ. The result is,

$$\tan 2\theta_s = -\frac{\sigma_x - \sigma_y}{2\tau_{xy}} \tag{2.15}$$

Where, $\theta_s = \theta_n \pm 45°$

Thus, making the corresponding maximum shear stress is equal to one-half the difference between the two principal stresses. While the normal stress where the shear stress occurs at both two orthogonal planes as in equation 2.17. Figure 2.8 shows the illustration of the transformation to the maximum shear stress direction.

$$\tau_3 = \sqrt{\left(\frac{\sigma_x + \sigma_y}{2}\right)^2 + {\tau_{xy}}^2} \tag{2.16}$$

$$\sigma_{\tau_3} = \frac{\sigma_x + \sigma_y}{2} \tag{2.17}$$

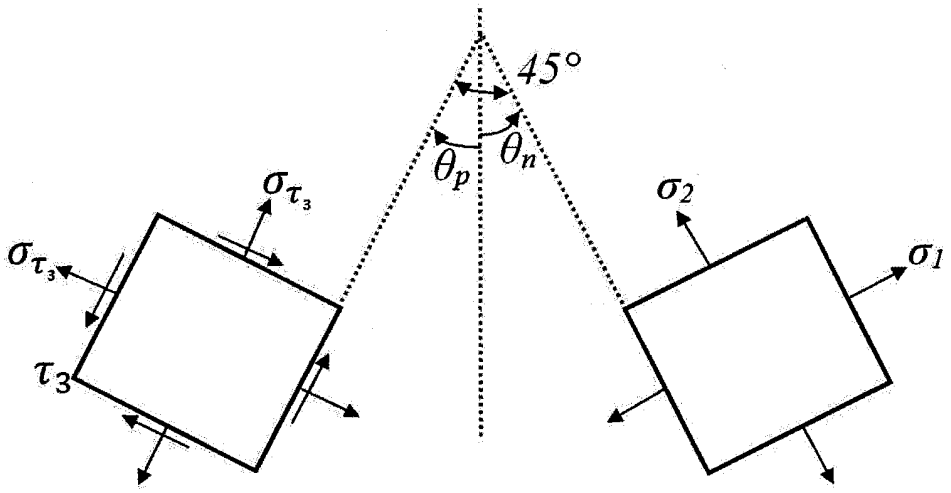

Figure 2.8: Transformation of an element to obtain the maximum shear stress direction

2.2.7 Principle Strain

Principle normal strains and principle shear strains occur in a similar manner as for principal stresses. Detailed analysis by Federick & Chang, 1972 in their book gives

equations that are identical to those for stresses except that shear strains are divided by two (Dowling, 2006). This statement means

$$\sigma_x, \sigma_y, \sigma_z = \varepsilon_x, \varepsilon_y, \varepsilon_z \tag{2.18}$$

$$\tau_{xy}, \tau_{yz}, \tau_{zx} = \frac{\gamma_{xy}}{2}, \frac{\gamma_{yz}}{2}, \frac{\gamma_{zx}}{2} \tag{2.19}$$

This will apply in general and to the special case where the, *x-y-z* axes are axes of the principal strain, *1-2-3*. For plane strain, where $\varepsilon_z = \gamma_{yz} = \gamma_{zx} = 0$, the axis of rotation and values for the principal normal strains would be;

$$\tan 2\theta_n = \frac{\gamma_{xy}}{\varepsilon_x - \varepsilon_y} \tag{2.20}$$

$$\varepsilon_1, \varepsilon_2 = \frac{\varepsilon_x + \varepsilon_y}{2} \pm \sqrt{\left(\frac{\varepsilon_x - \varepsilon_y}{2}\right)^2 + \frac{\gamma_{xy}}{2}^2} \tag{2.21}$$

Similarly, modified axis of rotation and principle shear stress gives for strains equations as in equation 2.22 through 2.24. With similar angle notation of principle stress which makes the θ is positive in counterclockwise (CCW). The positive normal strains corresponds to extension and negative corresponds to contraction. Positive shear strain causes a distortion corresponding to a positive shear stress such that the long diagonal parallelogram has a positive slope.

$$\tan 2\theta_s = -\frac{\varepsilon_x - \varepsilon_y}{\gamma_{xy}} \tag{2.22}$$

$$\gamma_3 = \sqrt{\left(\varepsilon_x - \varepsilon_y\right)^2 + \left(\gamma_{xy}\right)^2} \tag{2.23}$$

$$\varepsilon_{\gamma^3} = \frac{\varepsilon_x + \varepsilon_y}{2} \tag{2.24}$$

2.3 Contact mechanisms and mechanics

According to Holmberg *et al.* (2005), there were several types of tribological contact mechanisms. One of it is the macromechanical and another is micromechanical. Macromechanical contacts mechanisms will shows the friction and wear activities of the coatings by taking the strain distribution of the whole contact, the elastic and plastic deformation of whole contact results, and total wear of the particle formation with its dynamics.

Micromechanical contacts in the other hand, describes the crack initiation and propagation, material emancipation and particle formation. Shear and fracture mechanism are those two basics mechanisms of the crack nucleation and propagation (Holmberg *et. al*, 2009). Either way within the micromechanical contacts, there are several different mechanisms of coating failures such as extreme plastic deformation and rolling contact fatigue (Oliveira & Bower, 1996).

Contact mechanics have been studied since 1882 and were started with the publication of Heinrich Hertz. A contact is formed when two solid bodies were brought together. While contact mechanics is concerned with the stresses and deformations which came from the surface of those two bodies in contact (Johnson, 1985).

2.3.1 Types of contact

There are two types of contact, which is a conforming contact, and non-conforming contact. Conforming contact is called when the surfaces of those two bodies touch each other exactly together without any deformation. As an example, a flat slider bearing and journal bearing are said to be conforming contact. Bodies which do not have similar profiles are said to be non-conforming. If the bodies brought together without deformation, they will touch together which called point contact, if it is a point or line contact if it is a continuous line. An example of non-conforming contact is, a ball that makes point contact with the races in a ball bearing and whereas in a roller bearing the roller makes line contact.

When two non-conforming solid bodies are brought into contact, at the start they touch at a sole point. Under the slightest load applied, the bodies deformed in the area of their point of first contact so that they touch over an area which is finite

though small compared with the dimensions of the area contact and how it grows in size with increasing load (Johnson, 1985). The simple way to know the contact area of two-dimensional problem, the semi-width of the coating will be used as in Figure 2.9.

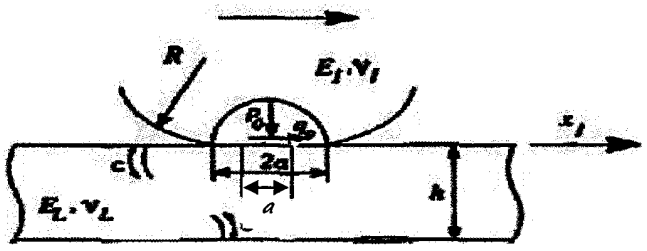

Figure 2.9: Contact semi-width of coating
(Oliveira & Bower, 1996)

2.3.2 Contact between a sphere and an elastic half-plane

An elastic sphere of radius, R indents an elastic half-space to depth, d and thus creates a contact area of radius

$$a = \sqrt{Rd} \tag{2.25}$$

The applied force F is related to the displacement d by

$$F = \frac{4}{3} E^* R^{1/2} d^{3/2} \tag{2.26}$$

Where

$$\frac{1}{E^*} = \frac{1-\nu_1^2}{E_1} + \frac{1-\nu_2^2}{E_2} \tag{2.27}$$

And E_1, E_2 are the elastic modulus and ν_1, ν_2 the Poisson's ratios associated with each body.

2.3.3 Concentrated normal force on a (2D) half-plane

A starting point for solving contact problems is to understand the effect of a "point-load" applied to an isotropic, homogeneous, and linear elastic half-plane, shown in the figure to the right. The problem may be either plane stress or plane strain. This is a boundary value problem of linear elasticity subject to the traction boundary conditions:

$$\tau_{xz}(x,0) = 0 \tag{2.28}$$

$$\sigma_z(x,z) = -P\delta\,(x,z) \tag{2.29}$$

Where $\delta(x, z)$ is the Dirac delta function. The boundary conditions state that there are no shear stresses on the surface and a singular normal force, P is applied at (0, 0). Applying these conditions to the governing equations of elasticity produces the result:

$$\sigma_x = -\frac{2P}{\pi}\frac{x^2 z}{(x^2+z^2)^2} \tag{2.30}$$

$$\sigma_z = -\frac{2P}{\pi}\frac{z^3}{(x^2+z^2)^2} \tag{2.31}$$

$$\tau_{xz} = -\frac{2P}{\pi}\frac{xz^2}{(x^2+z^2)^2} \tag{2.32}$$

For some point, (x, y) in the half-plane. The circle shown in the Figure 2.10 indicates a surface on which the maximum shear stress is constant. From this stress field, the strain components and thus the displacements of all material points may be determined.

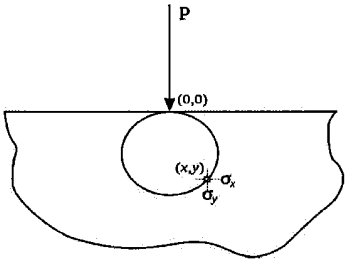

Figure 2.10: Concentrated pressure into contact of half-plane
(Johnson, 1985)

2.3.4 Distributed normal and tangential traction

Suppose, rather than a point load, P a distributed load $p(x)$ and tangential traction $q(x)$ is applied to the surface instead, over the range $-b < x < a$ as shown in Figure 2.11.

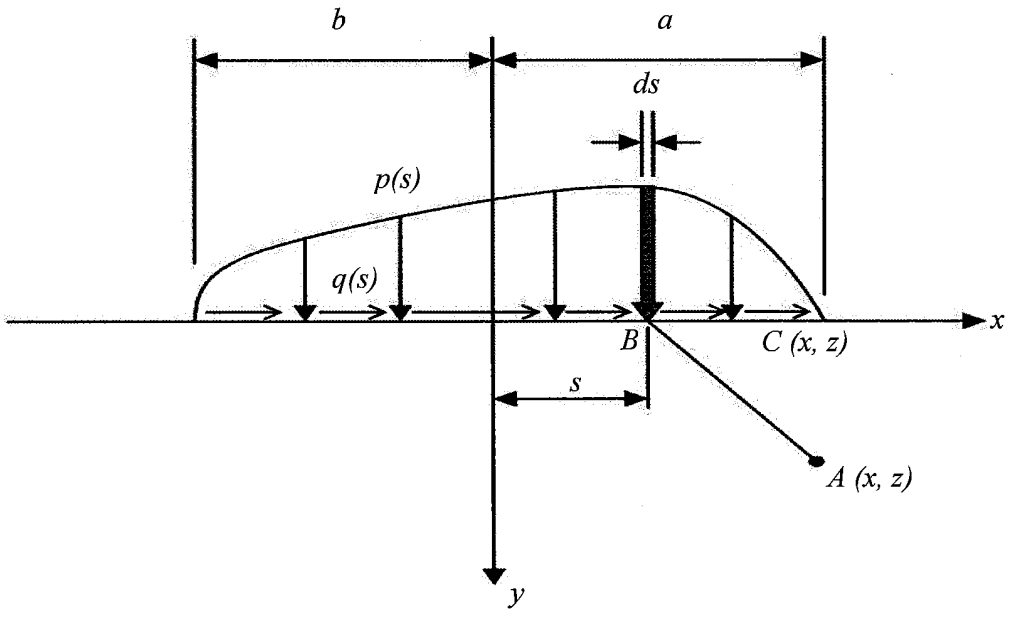

Figure 2.11: Normal pressure and tangential traction on contact half-plane
(Johnson, 1985)

These kinds of tractions would tend to arise as a result of friction. The principle of linear superposition can be applied to determine the resulting stress field as the solution to the integral equations:

$$\sigma_x = -\frac{2z}{\pi}\int_{-b}^{a}\frac{p(s)(x-s)^2 ds}{[(x-s)^2+z^2]^2} - \frac{2z}{\pi}\int_{-b}^{a}\frac{q(s)(x-s)^3 ds}{[(x-s)^2+z^2]^2} \quad (2.33)$$

$$\sigma_z = -\frac{2z^2}{\pi}\int_{-b}^{a}\frac{p(s) ds}{[(x-s)^2+z^2]^2} - \frac{2z^2}{\pi}\int_{-b}^{a}\frac{q(s)(x-s) ds}{[(x-s)^2+z^2]^2} \quad (2.34)$$

$$\tau_{xz} = -\frac{2z^3}{\pi}\int_{-b}^{a}\frac{p(s)(x-s) ds}{[(x-s)^2+z^2]^2} - \frac{2z}{\pi}\int_{-b}^{a}\frac{q(s)(x-s)^2 ds}{[(x-s)^2+z^2]^2} \quad (2.35)$$

2.3.5 Contact stress field

Contact stress field at the crack tip were altered if there is an elastic mismatch between coating and substrate. Greatest tensile stress occurs just above the interface between coating and substrate (Gupta & Walowit, 1974). There are two regions in the coating that are subjected to large tensile stress. First is at the surface immediately behind the contact and another is on the axis of symmetry at the interface between coating and substrate (Oliveira & Bower, 1996).

Increasing stiffness of coating relative to the substrate will also results in increasing of tensile stress at interface and also the coating layer thickness (Oliveira & Bower, 1996). This coating stress fields is then computed and later, the stress intensity factor was determined. Both of those results with a proper fracture criterion will then make able to predict the critical load to initiate fracture in the solid.

2.4 Ceramic coatings

There are huge assortments of ceramic coatings that can be useful to coat metal components in order to improve their practical properties. Most ceramic coatings are non-conductive to electrical current which makes them as an excellent choice for insulation purposes. It also has a notably higher level of abrasion resistance than most metals, and capable to maintain their integrity under severely elevated temperatures which sometimes up to 4,500 °F.

Ceramic coatings are regularly used as barrier materials to improve the contact between moving metal parts, such as in the automotive industry. However,

they are also progressively being in use to enhance certain manufacturing processes, and demonstrate potential for improving the effectiveness of some fabricating methods.

Ceramic materials, such as magnesium zirconate and zirconia, exhibiting a high level of hardness, thermal resistance, and elevated melting points are being used as heat barrier coatings for industrial parts.

2.4.1 Tungsten carbide coating

Industry that has a high demand for tungsten carbide is the military. This material is an important ingredient in the production of armor-piercing ammunition.

Though, it is not just the military and the heavy industries that have utilized for tungsten carbide. It also has a variety of domestic and civilian uses. Take for example the rolling tip of the usual ballpoint pen. That tip is usually made of tungsten carbide, as it helps diffuse the ink. Filaments used in light bulbs are also made out of tungsten carbide because of its heat-resistance qualities.

Tungsten carbide coatings are widely used to protect surfaces from wear in many types of applications. The wear behavior in any purpose is strongly influenced by the basic physical and mechanical properties of such coatings. Fracture toughness as a mechanical property indicates the resistance to fracture in the presence of a sharp crack, and thus provides a measure of the fundamental strength of the cemented carbides coatings.

2.4.2 Influence of coating thickness and hardness

It is known widely, that the coating surface thickness affects the coating toughness in. In hard coating system, coating layer thickness becomes an important controllable variable in design for crack suppression (Pajares *et. al.*, 1996). According to Babu *et. al.* (1996), the fracture resistances of the coating-substrate interface decreases as the coating thickness increases.

Generally, the acted *critical load,* $P_{fracture}$ on the coating layer is the interest in order to determine the coating fracture or delamination rather than *contact pressure,* P_{max} (Oliveira & Bower, 1996). Suppose, if a brittle and hard coating is applied on a ductile substrate and the coating layer is loaded by a rigid cylinder with a radius, R.

Thus, according to Oliveira & Bower (1996), the coating fracture or delamination is the dominant of failure mechanism. So, one need to calculate the maximum load $P_{fracture}$ that the coating can withstand without fracture. This will be discussed later. The fracture load is strongly influenced by the elastic mismatch and coating layer thickness, t_c.

2.5 Fracture mechanics

From a macroscopic view, a crack is seen to be as a cut in a body. There are two boundaries of a crack. One is the crack surfaces or also known as crack faces. Generally, these crack faces are traction-free. Another boundary is the crack front or some called as crack tip. Figure 2.12 shows a model of a cracked body.

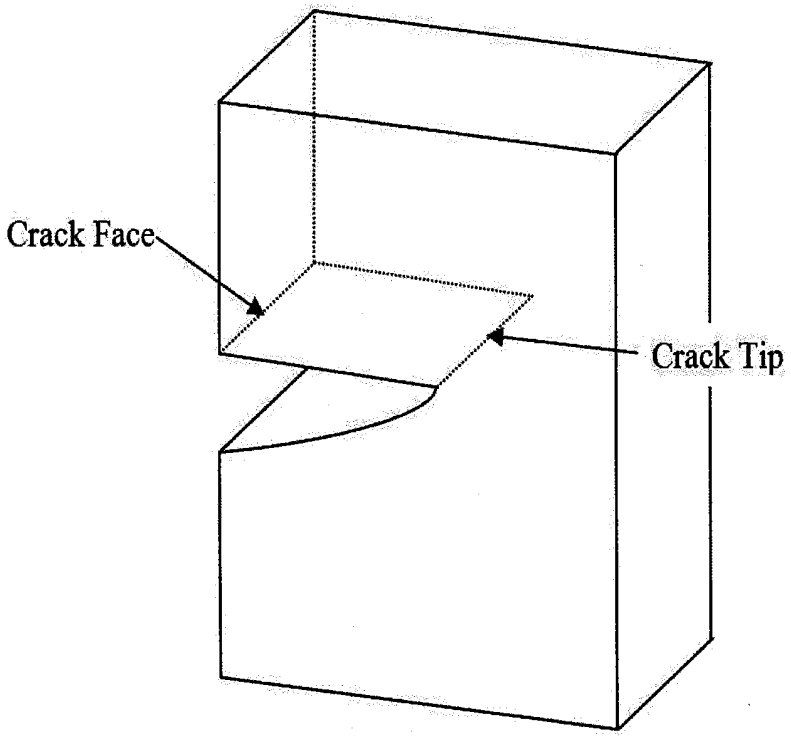

Figure 2.12: Cracked body

To discuss about the crack deformation, there are three modes of crack opening. Mode-I is a symmetrically crack opening on *y-plane* with the respect to the *x-* and *z-plane.* Mode-II is known as anti-symmetric crack opening of crack due to

relative displacement in x-direction which is normal to the crack front. Mode-III describes a separation due to relative displacement in *z-direction* which is tangential to the crack front. Typically Mode-III only involved in a three-dimensional analysis. But for the project due to only two-dimensional modelling is used, Mode-III fracture is neglected. Figure 2.13 shows the deformation for Mode-I, Mode-II, and Mode-III crack opening.

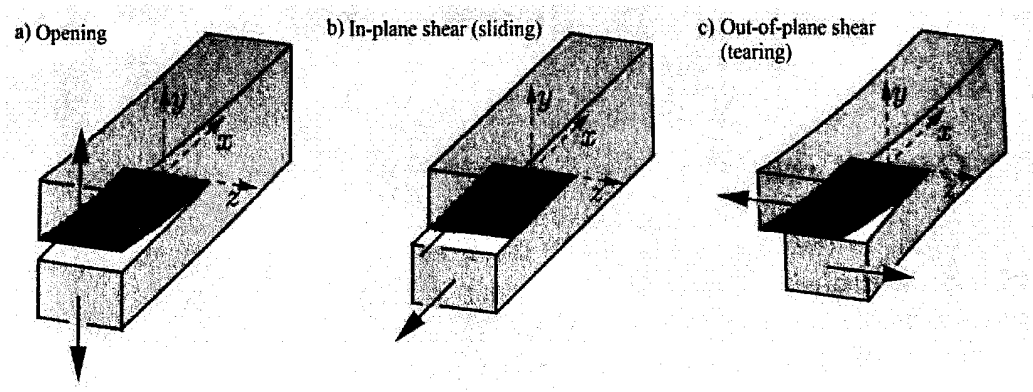

Figure 2.13: Crack opening for (a) Mode-I; (b) Mode-II; (c) Mode-III (Gross & Seelig, 2006)

In the knowledge of linear fracture mechanics, crack body is regarded as linear elastic in the whole region. So, any possibility of inelastic within or outside the process zone around the crack tip must be restricted to a small region which can be neglected from a macroscopic viewpoint (Gross & Seelig, 2006).

2.5.1 The *K-concept* (stress intensity factor)

The corresponding crack-tip field is fully characterized by the stress intensity factor K_I. This K_I-determined field dominates in an outwards limited region around the crack tip. Figure 2.14 shows the schematic with circle of radius R.

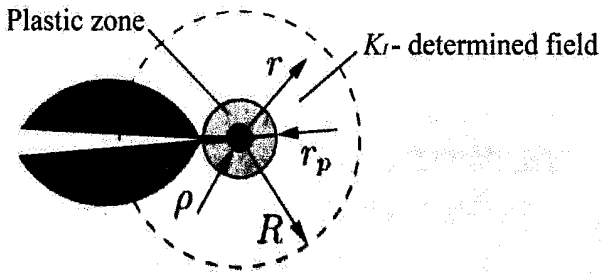

Figure 2.14: The *K-concept*

The process zone is denotes as ρ, and the plastic zone denotes as r_p Outside of R is the higher-order terms that cannot be neglected. Due to linear elasticity does not provide a realistic description of the actual stress and deformation state below a certain limit of r, the validity of the K_I-determined field is limited and also inwards. This is because of, there is no material that can bare an infinite stresses. Most of material, the plastic deformation happens at the crack tip when a strongly increasing stresses are taken into account.

From Figure 2.14, it is clearly shown that K_I-determined field is larger compared to inner domain. Under these conditions, it may be assumed that the process within the inner domain is controlled by the surrounding K_I-determined field. This hypothesis is the root reasoning of *K-concept* which is, the state within the crack tip can be characterized as K_I (Gross & Seelig, 2006). The stress intensity factor, K is considered to be a state variable of the region which is close to the crack tip.

Until then, the stress intensity factor can now be used to formulate the fracture criterion. In view of that, crack will propagates when stress intensity factor, K_I reaches a material specific critical value, K_{IC}.

$$K_I = K_{IC} \tag{2.36}$$

Under these conditions, a critical state exists at the crack tip which will soon cause material separation. Previously, an assumption was made that the state at the crack tip is determined by the actual value of K_I and does not depend on the loading records of the crack tip.

2.5.2 Fracture toughness of coating

The fracture toughness, K_{IC} of a material varies and strongly dependent on a number of influence parameters with appropriate experiments (Gross & Seelig, 2006). The interface between coating layer and substrate contains flaws. Generally, the interface has a fracture toughness which is less than that of either coating layer or substrate. The state of stress near the tip of a micro-crack is assumed to be characterized by mixed-mode (Mode I and Mode II) stress intensity factors K_I and K_{II}.

The intensity of the greatest tensile hoop stress was used as a mixed-mode fracture criterion. The plane strain fracture toughness K_{IC} was used to parameterize the fracture resistance of the solid. The maximum principal stresses at crack tip occur at an angle is

$$\theta_0 = \frac{3K_{II}^2 \pm K_I(8K_{II}^2 + K_I^2)^{1/2}}{89 + K_I^2} \tag{2.37}$$

Thus, the intensity factor will be

$$K_\sigma = \cos\frac{\theta_0}{2}\left\{K_I cos^2\frac{\theta_0}{2} - \frac{3}{2}K_{II}sin\theta_0\right\} \tag{2.38}$$

2.5.3 Fracture load

Fracture load is very sensitive to the coefficient of sliding friction and to the initial flaw size in the solid (Oliveira & Bower, 1996). To know the value of fracture load, one needs to know the value of stress intensity factor, K. As discussed previously, the fracture load influences the initiation of delamination of the coating.

It is proven by Oliveira & Bower (1996) that the mismatch of elasticity between coating and substrate increases when the fracture load decreases. The same author also shows that as the crack length increases, the fracture load will decrease. But if the crack length reaches a critical length, the fracture load value begins to fluctuate rapidly.

The crack length affects the tensile stress and crack tip intensity factor. Yet, when the length increases, the crack tip eventually experienced compressive stress

REFERENCES

A. L. Mohd Tobi, P. H. Shipway, S. B. Leen. (2013). Finite element modelling of brittle fracture of thick coatings under normal and tangential loading. *Tribology International, 58*, 29-39.

A. Pajares, L. Wei, B. R. Lawn, C. C. Berndt. (1996). Contact damage in alumina-based plasma sprayed coatings. *Journal of the American Ceramic Society, 79*, 1907-1914.

Dietmar Gross & Thomas Seelig. (2006). *Fracture Mechanics: With an Introduction to Micromechanics.* (F. F. Ling, Ed.) The Netherlands: Springer-Verlag Berlin Heidelberg.

F. Erdogan & M. Ozturk. (1995). Periodic cracking of functionally graded coatings. *Internation Journal of Engineering and Science, 33*, 2179-2195.

G. Kirchoff, Th. Gobel, H. -A Bahr, H. Balke, K. Wetzig, K. Bartsch. (2004). Damage analysis for thermally cycled (Ti,Al)N coatings - estimation of strentgh and interface fracture toughness. *Surface and Coating Technology, 179*, 39-46.

J. M. Leroy & B. Villechaise. (1990). Paper VIII (i) Stress determination in elastic coatings and substrate under both normal and tangential loads. *Tribology Series, 17*, 195-201.

K. Holmberg, A. Laukkanen, H. Ronkainen, K. Wallin. (2005). Tribological analysis of fracture conditions in thin surface coatings by 3D FEM modelling and stress simulations. *Tribology International, 38*, 1035-1049.

K. Holmberg, A. Laukkanen, H. Ronkainen, K. Wallin. (2009). Surface stresses in coated stell surfaces - influence of a bond layer on surface fracture. *Tribology International, 42*, 137-148.

K. L. Johnson. (1985). *Contact Mechanics.* Cambridge, United Kingdom: Cambridge University Press.

Lee Kee Sung. (2003). Effect of elastic modulus mismatch on the contact crack initiation in hard ceramic coating layer. *KSME International Journal, 17*, 1928-1937.

M. Vijaya Babu, R. Krishna Kumar, O. Prabhakar, N. Gowri Shankar. (1996). Fracture mechanics approaches to coating strength evaluation. *Engineering Fracture Mechanics, 55*, 235-248.

Norman E. Dowling. (2007). *Mechanical behavior of materials* (3rd ed.). New Jersey: Pearson-Prentice Hall.

P. K. Gupta & J. A. Walowit. (1974). Contact stress between an elastic cylinder and a layered elastic solid. *Journal of Librication Technology-Transaction of the ASME, 94*, 250-257.

R. B. King & T. C. O'Sullivan. (1987). Sliding contact stresses in a two dimensional layered elastic half-space. *International Journal of Solids and Structures, 23*(5), 581-597.

R. Kouitat Njiwa & J. Von Stebut. (1999). Boundary element numerical modelling as a fracture engineering tool: application to very thin coatings. *Surface and Coatings Technology, 116-119*, 573-579.

S. A. G. Oliveira & A. F. Bower. (1996). An analysis of fracture and delamination in thin coatings subjected to contact loading. *Wear, 198*, 15-32.

T. Belytschko & T. Black. (1999). Elastic crack growth in finite elements with minimal remeshing. *International Journal for Numerical Methods in Engineering, 45*, 601-620.